# Spectroscopy on the B850 Band of Individual Light-Harvesting 2 Complexes of *Rhodopseudomonas acidophila* I. Experiments and Monte Carlo Simulations

M. Ketelaars,* A. M. van Oijen,† M. Matsushita,† J. Köhler,‡ J. Schmidt,† and T. J. Aartsma*
*Department of Biophysics and †Centre for the Study of Excited States of Molecules, Huygens Laboratory, Leiden University, 2300 RA Leiden, The Netherlands; and ‡Experimental Physics IV, University of Bayreuth, 95440 Bayreuth, Germany

ABSTRACT The electronic structure of the circular aggregate of 18 bacteriochlorophyll *a* (BChl *a*) molecules responsible for the B850 absorption band of the light-harvesting 2 (LH2) complex of the photosynthetic purple bacterium *Rhodopseudomonas acidophila* has been studied by measuring fluorescence-excitation spectra of individual complexes at 1.2 K. The spectra reveal several well-resolved bands that are obscured in the single, broad B850 band observed in conventional absorption measurements on bulk samples. They are interpreted consistently in terms of the exciton model for the circular aggregate of BChl *a* molecules. From the energy separation between the different exciton transitions a reliable value of the intermolecular interaction is obtained. The spectra of the individual complexes allow for a distinction between the intra- and the intercomplex disorder. In addition to the random disorder, a regular modulation of the interaction has to be assumed to account for all the features of the observed spectra. This modulation has a $C_2$ symmetry, which strongly suggests a structural deformation of the ring into an ellipse.

## INTRODUCTION

Significant progress has been made in photosynthesis research by resolving the structures of isolated pigment-protein complexes, especially those that form the building blocks of the photosynthetic apparatus of purple bacteria. As more structural data become available, new questions can be addressed, ranging from details of intermolecular interactions to the supramolecular organization of the entire apparatus. In the past few years a significant research effort was directed toward the investigation of the light-harvesting 2 (LH2) complex of the photosynthetic purple bacterium *Rhodopseudomonas (Rps.) acidophila*, stimulated by the resolution of the three-dimensional structure of this complex (McDermott et al., 1995). The structure was found to be highly symmetric with $C_9$, ninefold rotational symmetry.

Fundamental aspects of light-harvesting complexes in general, and of LH2 in particular, are the nature and strength of the intermolecular interactions and the manifestation of these interactions in the spectroscopic and functional properties of the system. From this perspective, LH2 is an important test case for several reasons. First, reasonable estimates of the strength of the intermolecular interactions can be calculated from the structure. Second, there are only three inequivalent binding sites for bacteriochlorophyll *a* (BChl *a*) molecules, which reduces the ambiguity in the assignment of site energies and interactions. Last but not least, phenomena associated with cooperativity of optical excitations will be much more pronounced because of the high symmetry, and thus more easily discernible. As a matter of fact, the high symmetry of the LH2-type complexes has a dominant effect on the nature and characteristics of the optically excited states (Sauer et al., 1996; Wu and Small, 1997). For these reasons, the LH2 complex offers the unique opportunity of directly comparing theoretical predictions with experimental spectroscopic observations.

So far, isolated LH2 complexes have been studied intensively using many different optical techniques; for an extensive review and discussion, see Sundström et al. (1999). Different methods of steady-state spectroscopy have been applied to study in detail many aspects of the optical spectrum (De Caro et al., 1994; Beekman et al., 1997; Koolhaas et al., 1997, 1998). In addition, much work was focused on the excited-state dynamics of LH2 (Hess et al., 1993; Pullerits et al., 1994; Du et al., 1994; Monshouwer et al., 1995; Joo et al., 1996; Jimenez et al., 1997; Kennis et al., 1997a; Zhao et al., 1999; Polivka et al., 2000). A recurring theme in many discussions in the literature is the nature of the electronically excited states, and in particular the degree of delocalization of the optical excitation (Monshouwer and van Grondelle, 1996; Pullerits et al., 1996; Monshouwer et al., 1997; Chachisvilis et al., 1997; Kennis et al., 1997b; Novoderezhkin et al., 1999). Despite this considerable effort, as yet it has proven difficult to analyze this system in all its detail. This is caused mainly by the pronounced disorder in these types of systems, which masks details in the steady-state optical spectra, even at low temperature. One way to eliminate this complication is to apply the technique of single-molecule spectroscopy to study individual LH2 complexes (Bopp et al., 1997; Tietz et al., 1999; van Oijen et al., 1999a).

*Received for publication 28 August 2000 and in final form 19 December 2000.*

Address reprint requests to Dr. M. Ketelaars, Leiden University, Department of Biophysics, Huygen Laboratory, Niels Bohrweg 2, 2333 CA Leiden, The Netherlands. Tel.: 31-71-5275983; Fax: 31-71-5275819; E-mail: ketelaars@biophys.leidenuniv.nl.

© 2001 by the Biophysical Society

0006-3495/01/03/1591/13 $2.00

Recently we succeeded in studying individual LH2 complexes at low temperature (van Oijen et al., 1998, 1999a,b, 2000). The spectra observed for the B800 pigment pool of LH2 provided, for the first time, direct and detailed insight in the electronic structure of this part of the complex. The polarization dependence of the narrow lines around 800 nm indicate a strong localization of the electronically excited states on the individual BChl *a* molecules in the B800 ring. In addition, the spectral heterogeneity could be described as arising from intracomplex and intercomplex disorder (van Oijen et al., 2000). On the other hand, the spectra associated with the B850 pigment pool showed a completely different behavior. The observed broad spectral lines were interpreted in terms of an exciton energy level scheme, and the structure in the B850 band was consistent with the assumption that the excited states are almost completely delocalized. Furthermore, from the characteristic patterns observed in the spectra, it was inferred that the LH2 complex in its ground state is subjected to an elliptical deformation (van Oijen et al., 1999a).

In a series of two papers, we present a more detailed analysis of the fluorescence-excitation spectra of the B850 band of single LH2 complexes of *Rps. acidophila* on the basis of an exciton model for the excited states of the circular aggregate of the 18 BChl *a* pigments. In this paper we will focus on the experimental observations and how they relate to the electronic structure. The observed spectral features can be explained consistently by assuming a random disorder of the excitation energy of the individual pigments and a modulation of the interaction energies with a $C_2$ symmetry caused by a static deformation of the ring into an elliptical shape. The effect of such an elliptical deformation on the electronic structure and on the single-molecule spectra is examined in more detail from a theoretical point of view in the accompanying paper (Matsushita et al., 2001).

## THEORY

The basic building block of LH2 is a protein heterodimer, $\alpha\beta$, which binds three BChl *a* molecules and one carotenoid molecule. The LH2 complex of *Rps. acidophila* consists of nine of such $\alpha\beta$ polypeptide heterodimers. A very pronounced feature of the complex is the fact that, at least in crystalline form, this complex has a $C_9$, ninefold rotational symmetry (McDermott et al., 1995). Two BChl *a* pigment pools can be distinguished and are labeled B800 and B850, according to their room temperature absorption maxima in the near infrared. The B800 ring consists of nine pigments, which have their molecular plane perpendicular to the symmetry axis. The B850 ring consists of nine repeating pairs of $\alpha$- and $\beta$-bound pigments, which are tightly organized like the blades of a turbine with their molecular planes parallel to the symmetry axis (Fig. 1).

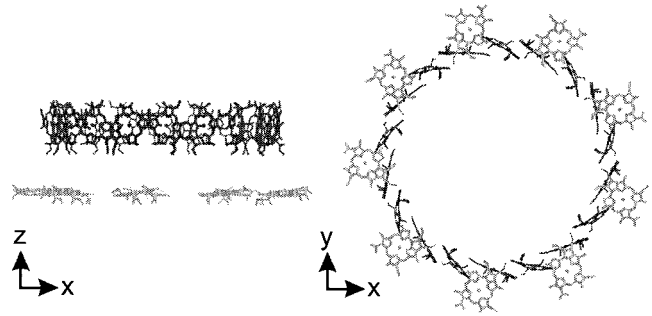


FIGURE 1 Geometrical arrangement of the 27 BChl *a* pigments of the LH2 complex of *Rps. acidophila*. The B800 pigments are depicted in light gray and the B850 pigments in black. The phytol chains are omitted for clarity. The complex has a ninefold circular symmetry with the $C_9$ symmetry axis parallel to the *z* axis and coinciding with the cylindrical axis of the complex. Data were obtained from the Brookhaven Protein Data Bank (1kzu.pdb).

To describe the spectroscopic properties of the B850 ring, two parameters are important: the site energies of the individual B850 pigments and their intermolecular interactions. With the term "site energy" we indicate the $Q_y$ transition energy of the individual pigments in zero order, i.e., in the absence of interactions between the pigments. The intermolecular interactions between the B850 pigments can be calculated from the structure parameters of the $C_9$ symmetric ring. The simplest approach is to use the point-dipole approximation to describe the transition-dipole interaction. Since the closest distance between the pigments is rather small, the validity of this approximation may be questioned; therefore, other approaches have been taken as well. For example, a point-monopole treatment (Sauer et al., 1996) and the transition density cube method (Krueger et al., 1998) were applied to include a spatial distribution of the transition dipole, whereas quantum-theoretical calculations were able to take exchange interactions into account (Alden et al., 1997; Scholes et al., 1999).

The spectroscopic properties of the B850 ring are determined by its electronic structure. This structure can be described using the following Hamiltonian for a single excited Frenkel exciton:

$$H = \sum_{n=1}^{18} (E_{0,n} + \Delta E_n)|n\rangle\langle n| + \sum_{n=1}^{18} (V_{0,n} + \Delta V_n)[|n\rangle n + 1| + H.c.] + \sum_{n=1}^{18} (W_{0,n} + \Delta W_n)[|n\rangle\langle n + 2| + H.c.] \quad (1)$$

where $E_{0,n}$ denotes the site energies of the individual pigments and $V_{0,n}$ and $W_{0,n}$ are the nearest- and second-neigh-

bor interactions, respectively. In the present work the interpigment interactions are taken into account up to the second neighbors. Static disorder gives rise to local variations in the protein environment of the binding sites, causing a shift $\Delta E_n$ of the site energies for each pigment. Usually, a Gaussian distribution of site energies is used to model this type of diagonal disorder. Any structural disorder or deformation in the ring will cause deviations from the perfect $C_9$ symmetry and results in a variation of the interactions, represented by $\Delta V_n$ and $\Delta W_n$. This disorder is referred to as off-diagonal disorder.

In Eq. 1 it is assumed that the different participating pigments are characterized by only a single electronic transition. The interactions of the B850 with the B800 pigments are ignored. This is justified by the fact that the interactions with the B800 pigments are much smaller owing to the larger center-to-center distance. In addition, the energy difference between the respective $Q_y$ transitions greatly reduces the influence of the B800 ring on the excited states of the B850 absorption (Sauer et al., 1996). Electron-phonon coupling is also neglected, i.e., we assume that the optical spectra are dominated by the 0–0 transition of the $Q_y$ band of the B850 pigments. This assumption is not unreasonable in view of the weak electron-phonon coupling of the B800 pigment, as observed in the fluorescence-excitation spectra of individual complexes (van Oijen et al., 1999b). Other BChl *a*-containing complexes, most notably the FMO complex, also exhibit weak electron-phonon coupling (Vulto et al., 1999a). Time-dependent exciton localization is not important at 1.2 K, because the (thermal) phonon population required for this effect is negligible. Linear electron-phonon coupling at 1.2 K does play a role in downward transitions between exciton states, as demonstrated in the case of the FMO complex (Vulto et al., 1999a). This relaxation process occurs at a very short, subpicosecond timescale, so that it may be assumed that the fluorescence originates from the lowest energy state in the exciton manifold.

In order to take into account the dimerization in the ring, different site energies and interactions for the $\alpha$- and $\beta$-bound pigments must be introduced. As a dimer we choose the $\alpha\beta$ unit with the tail-tail configuration of the $Q_y$ transition-dipole moments (Sauer et al., 1996) (Fig. 2, top). $V_i$ and $V_e$ are the intra- and interdimer nearest-neighbor interactions, and $W_\alpha$ and $W_\beta$ are second-neighbor interactions between, respectively, the $\alpha$- and $\beta$-bound pigments. Due to the slightly different local environments of the $\alpha$- and $\beta$-bound pigments, the transition energies for these pigments are very likely to be different. Such a difference has been pointed out to be important for the simulation of the circular dichroism spectrum. It was concluded that the $\alpha$-bound pigments have a higher site energy than the $\beta$-bound pigments, where the difference is about the same as the average nearest-neighbor interaction (Koolhaas et al., 1997).

When we include the dimerization in the Hamiltonian of Eq. 1 and neglect the diagonal ($\Delta E_n$) and off-diagonal ($\Delta V_n$, $\Delta W_n$) disorder, the energies of the excited states of the

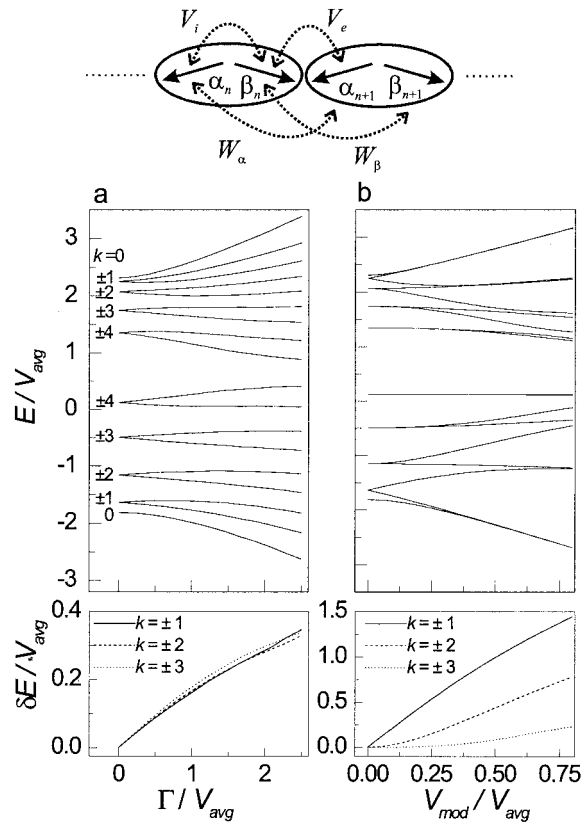


FIGURE 2 The upper part of the figure displays schematically the orientation of the transition-dipole moments of the individual BChl *a* molecules and their mutual interactions. For the unperturbed ring, the following parameters have been used: $E_\alpha = 240\ \text{cm}^{-1}$, $E_\beta = 0\ \text{cm}^{-1}$, $V_i = 250\ \text{cm}^{-1}$, $V_e = 230\ \text{cm}^{-1}$, $W_\alpha = W_\beta = -30\ \text{cm}^{-1}$. All energy scales are in units of $V_{avg}$ with $V_{avg} = (V_i + V_e)/2$. (*a*) Simulation of the excited state energies with different amounts of random diagonal disorder. The site energies are distributed according to a Gaussian distribution defined by a full width at half maximum ($\Gamma$) and centered on $E_\alpha$ and $E_\beta$. Energy values are averaged over 10,000 iterations. In the lower part of the figure the splittings for the $k = \pm1$ (*solid line*), $k = \pm2$ (*dashed line*), and $k = \pm3$ (*dotted line*) pairs are shown. (*b*) Simulation of the excited-state energies for different amplitudes of a $\cos(2\phi)$ modulation of the interactions between the pigments. The amplitude of the modulation is $V_{mod}$ for the nearest-neighbor and $W_{mod}$ for the second-neighbor interactions, where $W_{mod} = -V_{mod}/8$. The lower part of the figure depicts the splitting of the $k = \pm1$, $\pm2$, and $\pm3$ pairs.

unperturbed aggregate are given by (see Matsushita et al., 2001):

$$E_k^{\pm} = \bar{E} + 2\bar{W}\cos(k\delta) \pm \sqrt{[E_{\alpha\beta}/2 + W_{\alpha\beta}\cos(k\delta)]^2 + V_i^2 + V_e^2 + 2V_iV_e\cos(k\delta)}, \quad (2)$$

with

$$\bar{E} = (E_\alpha + E_\beta)/2, \quad E_{\alpha\beta} = (E_\alpha - E_\beta),$$
$$W = (W_\alpha + W_\beta)/2, \quad W_{\alpha\beta} = (W_\alpha - W_\beta), \quad (3)$$

where $\delta = 2\pi/9$ and $k$ the quantum number ranging from $0, \pm 1, \ldots, \pm 4$. $E_\alpha$ and $E_\beta$ are the excitation energies of the $\alpha$- and $\beta$-bound pigments, respectively. Due to the second-neighbor interaction, the overall manifold is asymmetric around $\bar{E}$.

The $Q_y$ transition-dipole moments of the monomers are oriented nearly in the plane of the ring structure resulting for the B850 assembly in a large in-plane component of the transition-dipole moment, which is concentrated exclusively in the $k = \pm 1$ degenerate pairs. The out-of-plane components of the monomer transition moments give rise to a small oscillator strength in the nondegenerate $k = 0$ level (Sauer et al., 1996; Alden et al., 1997). Since in the dimer unit both $Q_y$ transitions are oriented essentially anti-parallel, the optical transition to the lower dimer state is strongly allowed and that to the upper state is almost forbidden (see, e.g., Cantor and Schimmel, 1980). Consequently, nearly all the strength is concentrated in the $k = \pm 1$ states of the lower exciton manifold (Sauer et al., 1996; Alden et al., 1997). The two transition-dipole moment vectors within this degenerate pair are oriented perpendicular with respect to each other (Alden et al., 1997).

Random diagonal disorder, caused by stochastic variations in the protein environment, introduces the term $\Delta E_n$ in Eq. 1, and this has several effects on the exciton manifold (Dracheva et al., 1996; Monshouwer et al., 1997; Alden et al., 1997; Hu et al., 1997; Wu and Small, 1998; Freiberg et al., 1999). First, it causes mixing of the different exciton levels and redistributes oscillator strength to nearby states, including the $k = 0$ state. Therefore, despite the small oscillator strength of the $k = 0$ state, fluorescence of LH2 is readily observed (Monshouwer et al., 1997). Second, it modifies the spacing between the exciton levels and removes their pair-wise degeneracy. The latter effect is illustrated in Fig. 2 *a*, where a simulation is shown of the relative energies of the exciton states as a function of $\Gamma/V_{avg}$. Here, $\Gamma$ is the full width at half maximum (FWHM) of an assumed Gaussian distribution of site energies of the individual B850 molecules and $V_{avg}$ is the average nearest-neighbor interaction, $(V_i + V_e)/2$. This simulation is based on a Monte Carlo calculation averaged over 10,000 iterations, each with a random choice of site energies from the Gaussian distribution. As can be seen in the top part of the figure, diagonal disorder modifies the exciton level spacing, and changes the relative energy of all exciton levels. Each degenerate pair is split with the same value $\delta E$ and this splitting increases linearly for small values of diagonal disorder and nonlinearly for larger values. This is illustrated in the lower panel of Fig. 2 *a*, where $\delta E$ is plotted for the three lowest degenerate pairs of energy states ($k = \pm 1$, $\pm 2$, and $\pm 3$) as a function of $\Gamma$. Other authors reported similar results (Dracheva et al., 1996; Hu et al., 1997; Freiberg et al., 1999). When the ratio $\Gamma/V_{avg}$ is much larger than unity, the excitation will be localized on an individual pigment. In this regime, which applies, for instance, to the B800 pigment pool, the transition energies are distributed according to a Gaussian distribution with a FWHM of $\Gamma$. The transition from the delocalized exciton to the localized excitation is implicit in Fig. 2 *a*.

The random off-diagonal disorder described by the terms $\Delta V_n$ and $\Delta W_n$ in Eq. 1 is caused by the variations in the dipolar coupling between the BChl *a* pigments and originates from irregularities in the orientations and positions of the individual transition dipoles. Fidder et al. (1991) described this kind of disorder by a Gaussian distribution of the interaction strengths, in the case of J-aggregates. The effects on the exciton manifold are indistinguishable from the effects of random diagonal disorder. In our calculations we limit ourselves, therefore, to random diagonal disorder.

Several experimental observations (Bopp et al., 1999; van Oijen et al., 1999a) suggest that in the LH2 aggregate a regular modulation is present in the intermolecular interactions due to a deformation of the ring. Wu and colleagues (Wu et al., 1997; Wu and Small, 1997, 1998) have analyzed the effects of such regular modulations on the electronic structure of LH2. They showed that an arbitrary disorder could be expressed as a superposition of basis defect patterns, each transforming according to an irreducible representation of the $C_9$ point group. The four non-totally symmetric irreducible representations of the $C_9$ point group correspond to a modulation of the interaction with a periodicity determined by the quantum number $k = 1, 2, 3$, and 4. The selection rule for the matrix element of a $k = n$ type modulation between different $k$ states is $\Delta k = \pm n, \pm(9\text{-}n)$. Thus, the basic modulation that splits the $k = \pm 1$ states has $k = 2$. Such a modulation can be expressed as a $\cos(2\theta)$ modulation of both the nearest- and second-neighbor interaction energies, where $\theta$ corresponds to the angular position of the pigment in the ring. We thus have

$$\begin{aligned} H = & \sum_{n=1}^{18} (E_{0,n} + \Delta E_n)|n\rangle\langle n| \\ & + \sum_{n=1}^{18} \{V_{0,n} + V_{mod} \cos[2\phi(n + \tfrac{1}{2})]\} \\ & \times [|n\rangle\langle n+1| + H.c.] \\ & + \sum_{n=1}^{18} \{W_{0,n} + W_{mod} \cos[2\phi(n+1)]\} \\ & \times [|n\rangle\langle n+2| + H.c.] \end{aligned} \tag{3}$$

where $\phi = 2\pi/18$. $V_{mod}$ and $W_{mod}$ are the amplitudes of the modulation of, respectively, the nearest- and second-neighbor interactions.

The $\cos(2\theta)$, or $C_2$-type of perturbation couples only exciton states that have a difference of their quantum num-

ber of $\Delta k = \pm 2$. The dominant effect of this perturbation is the coupling between the degenerate $k = \pm 1$ states. Their degeneracy is lifted and in first approximation the energy splitting of the low $k = \pm 1$ pairs is equal to $2(V_{mod} + W_{mod})$ (Matsushita et al., 2001). The positions of the $k = \pm 1$ states is further affected by their interactions with the respective $k = \pm 3$ levels. However, this effect is much smaller than the former one due to the energy difference between the $k = \pm 1$ and $k = \pm 3$ states. This also applies to all the other interactions between the different $k$ levels.

In Fig. 2 *b*, the effect of a $C_2$-type modulation of the interaction energy on the exciton manifold is depicted as a function of the amplitude of this modulation. The amplitude $W_{mod}$ is taken to be 12% of $V_{mod}$ based on the assumption that $V_{mod}$ and $W_{mod}$ scale similarly to $V_{0,n}$ and $W_{0,n}$. As can be seen in the top part of the figure, the $C_2$-type modulation modifies the exciton level spacing in a completely different manner than the random diagonal disorder (Fig. 2 *a*). As expected, the size of the splitting, $\delta E$, is largest for $k = \pm 1$ and is much smaller for the $k = \pm 2$ and $k = \pm 3$ levels (Fig. 2 *b*, lower panel).

The $C_2$-type modulation also leads to a redistribution of the oscillator strength among the exciton states. Owing to the selection rule $\Delta k = \pm 2$, only the low energy $k = \pm 3$ states gain significant oscillator strength by their interaction with the $k = \pm 1$ states. Note that a $C_2$-type modulation alone does not give rise to an extra oscillator strength of the $k = 0$ state.

## MATERIALS AND METHODS

The LH2 complexes of *Rps. acidophila* (strain 10050) were prepared as described elsewhere (Kennis et al., 1997b). Hydrolyzed polyvinyl alcohol (PVA) (BDH British Drug House, Poole, England; Mw = 125,000) was purified over a mixed resin in order to remove ionic impurities (Lösche et al., 1987). A polymer-LH2 solution was prepared by adding 1% (wt/wt) purified PVA to a solution of $5 \times 10^{-11}$ M LH2 in buffer (10 mM Tris, 0.1% Lauryldimethylamine *N*-oxide, 1 mM EDTA, pH 8.0). A drop of this solution was spin-coated on a LiF substrate by spinning it for 15 s at 500 rpm and 60 s at 2000 rpm, producing high quality films with a thickness of $<1$ $\mu$m. The samples were mounted in a cryostat and cooled to 1.2 K.

To perform fluorescence microscopy and fluorescence-excitation spectroscopy, the samples were illuminated with a continuous-wave tunable Ti:Sapphire laser. A fluorescence-excitation spectrum of an individual LH2 complex was obtained in two steps. First, a wide-field image was taken of the sample by exciting at 800 nm and detecting fluorescence at 890 nm with a CCD camera. From this image a spatially well-isolated complex was selected. Next, a fluorescence-excitation spectrum of this complex was obtained by switching to the confocal mode of the setup and scanning the excitation wavelength, while detecting fluorescence at 890 nm with an avalanche photodiode. The detection bandwidth was 20 nm.

Since light-induced fluctuations of the fluorescence intensity on a time scale of seconds were observed (van Oijen et al., 1999a, 2000), the spectra were obtained by rapidly scanning the whole spectral range and storing the different traces separately. With a scan speed of the laser of 3 nm/s and an acquisition time of 10 ms per data point, this yields a nominal resolution of 0.5 $cm^{-1}$, ensuring that the spectral resolution is limited by the spectral bandwidth of the laser (1 $cm^{-1}$). For most spectra about 70 scans were added. For more experimental details, see van Oijen et al. (1999b).

To examine the polarization dependence of the spectra, a ½ λ plate was put in the confocal excitation path. For each individual complex six spectra were obtained at polarization intervals of 30°. A total of 19 complexes was studied.

The atomic coordinates of LH2 of *Rps. acidophila* were taken from the Brookhaven Protein Data Bank (1kzu.pdb). The electronic structure of the B850 ring of LH2 was approximated using only the lowest ($Q_y$) excited states of the individual BChl molecules. These $Q_y$ transition dipoles were assumed to be oriented along the axis running through the $N_I$-$N_{III}$ nitrogen atoms of the BChl. Note that these are the $N_B$-$N_D$ nitrogen atoms according to the crystallographic nomenclature.

To account for the deviation, $\Delta E_n$, of every BChl molecule from the average transition energy $E_0$, the site energies were randomly chosen from a Gaussian distribution defined by the center energy and a width $\Gamma$ (FWHM). From experimental studies of the B800 transition energies of individual LH2 complexes (van Oijen et al., 2000), as well as time-resolved pump-probe absorption difference spectra of the B850 band (Freiberg et al., 1999), it appears that we may consider two contributions to the distribution of site energies for the individual BChl *a* molecules. First, within each complex the 18 BChl *a* molecules will show variations of their site energy with respect to the spectral mean for this particular complex (intracomplex heterogeneity). Second, also the spectral mean for different complexes will be a distributed parameter (intercomplex heterogeneity). In order to take this into account, two Gaussian distributions were introduced defined by their FWHM: $\Gamma_{intra}$ and $\Gamma_{inter}$. Each complex had its own spectral mean chosen from the intercomplex distribution, and each BChl its own site energy from the intracomplex distribution, which was located around the respective center energy of the intercomplex distribution.

Monte Carlo simulations were performed, using 10,000 iterations to simulate the behavior of an ensemble of individual LH2 complexes.

## RESULTS

In Fig. 3, the fluorescence-excitation spectra of several individual LH2 complexes are compared. The upper trace shows the corresponding spectrum taken from a bulk sample (*dashed line*) together with the spectrum that results from the summation of all the spectra measured for individual complexes (*solid line*). The two spectra are in excellent agreement and both feature two broad structureless bands around 800 nm and 860 nm, corresponding to the absorptions of the B800 and B850 pigments of the complex. By measuring the fluorescence-excitation spectra of the individual complexes, remarkable features become visible which are otherwise buried under the ensemble average. In particular, a striking difference between the B800 and B850 bands becomes evident. The spectra around 800 nm show a wide distribution of narrow absorption bands, whereas in the B850 spectral region 2 to 3 broad bands are present. The analysis of the polarization dependence of the intensity of the B800 lines indicated that the excitations in this manifold are mainly localized on individual BChl *a* molecules. A detailed description of these results can be found elsewhere (van Oijen et al., 1999b, 2000). In all spectra of the B850 band, two broad absorption lines around 860 nm are observed. For 40% of the complexes these two lines are accompanied by a weaker transition at higher energy (Fig. 3). By exciting the complexes with linearly polarized light at different polarization angles, the relative orientation of the transition-dipole moments associated with the two

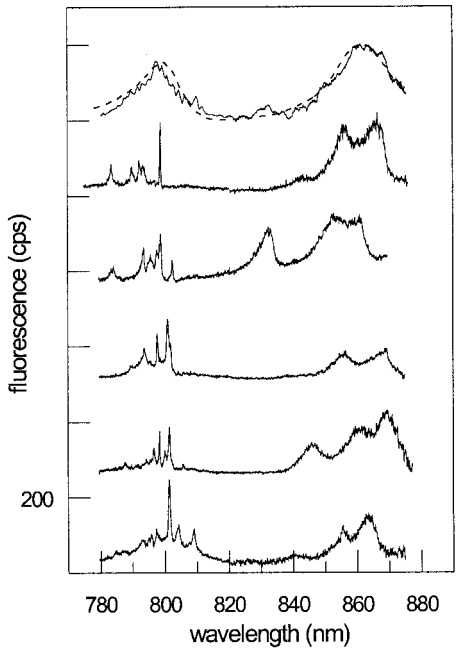


FIGURE 3 Fluorescence-excitation spectra of LH2 complexes of *Rps. acidophila*. The top traces show the comparison between an ensemble spectrum (*dashed line*) and the sum of 19 spectra recorded from individual complexes (*solid line*). For each complex, six individual spectra were summed that were obtained at different excitation polarizations. The lower five traces display spectra from single LH2 complexes. All spectra were measured at 1.2 K at 20 W/cm$^2$ with LH2 dissolved in a PVA-buffer solution. The individual spectra were taken from van Oijen et al. (1999a).

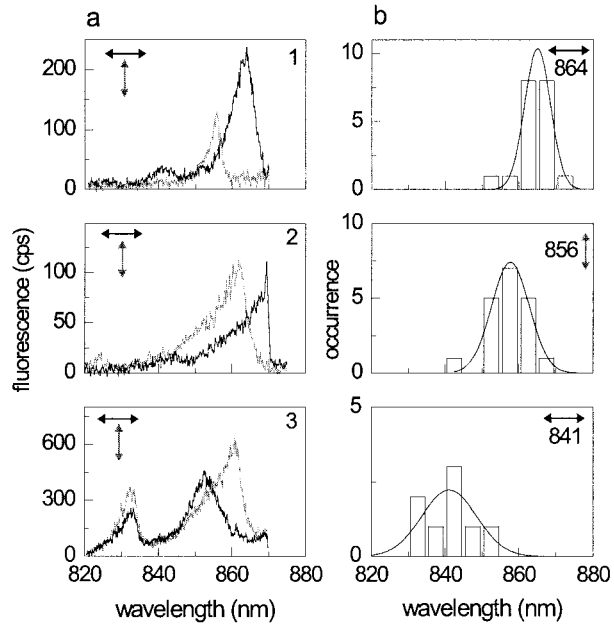


FIGURE 4 (*a*) Fluorescence-excitation spectra of the B850 spectral region of three individual LH2 complexes. For each complex, two spectra with mutually orthogonal polarization (*arrows*) of the excitation are shown. (*b*) Distribution of the spectral positions for 19 complexes of the three observed bands. The experimental conditions are the same as in Fig. 3.

prominent absorptions around 860 nm was determined. For all the complexes studied we found that these transition-dipole moments were mutually orthogonal (Fig. 4 *a*). The high-energy absorption band (Fig. 4 *a*, complex 3) appears to be homogeneous, and shows only a slight dependence of its total intensity on the polarization of the incoming beam.

Fig. 4 *b* depicts the distributions of the spectral positions of the three observed transitions. For the red absorption the distribution is centered at 864 nm. For the transition perpendicular to this one, the distribution is centered around 856 nm. The high-energy absorption present in some of the spectra is distributed around 841 nm, as can be seen in the lower panel of Fig. 4 *b*. The corresponding bands in the single-molecule spectra will be referred to as the 864, 856, and 841 nm bands, respectively. The average energy separation between this last transition and the spectral mean of the two mutually perpendicularly polarized transitions is 285 ± 35 cm$^{-1}$. The linewidths of the 864 and 856 nm absorption bands in the individual spectra range from 50 to 250 cm$^{-1}$, with an average value of 120 cm$^{-1}$. This corresponds to a value for the total dephasing time between 100 and 20 fs, in agreement with the ensemble averaged values reported for the B850 band at low temperature (Vulto et al., 1999b; Sundström et al., 1999).

The two prominent absorptions around 864 nm and 856 nm (Fig. 4 *b*) are assigned to the low energy $k = \pm 1$ exciton states, which agrees with their mutual orthogonal transition-dipole moments lying in the plane of the ring. The absorption around 841 nm (Fig. 4 *b*) is attributed to higher exciton states. The splitting of the $k = \pm 1$ states, as well as the appreciable oscillator strength of the higher exciton states, is ascribed to static energetic disorder in the individual LH2 complexes.

For all complexes we studied so far, it was possible to find a polarization of the incident excitation light such that either the 864 or the 856 band could be exclusively observed. Consequently, we conclude that the LH2 complexes are oriented within the PVA matrix with their $C_9$ axis perpendicular to the plane of the substrate at which the sample is deposited. This might result from the spin-coating procedure, which introduces a shear force in the film, in combination with the thickness of the film (<1 $\mu$m) after evaporation of most of the solvent. PVA layers that were prepared by simply spreading a drop of the LH2/PVA solution onto the substrate did not show a high degree of orientation.

A crucial check for the applicability of the exciton model to the B850 system would be observation of the $k = 0$ exciton state. The fluorescence lifetime of LH2 from *Rps. acidophila* is about 1 ns and corresponds to the decay time of the $k = 0$ level. Consequently, a relatively narrow absorption line is expected for this state. For three out of 19

complexes, we have indeed been able to observe such a line on the low energy side of the $k = \pm 1$ transitions. Rapid spectral diffusion smears out this line and hinders its experimental observability. Therefore, we modified the data acquisition in a way similar to that reported earlier (van Oijen et al., 2000). Repetitive scans of the B850 spectral region were recorded at a high scan rate (3 nm/s) and stored separately in computer memory. For each of these scans, the narrow line was fitted with a Lorentzian by which the peak position could be determined with reasonable accuracy. Subsequently, all data scans were spectrally shifted such that the peak positions coincided and were then added together. The resulting spectra, shown in Fig. 5, bring out the $k = 0$ transition very prominently because of this correction for the spectral diffusion effects, although other parts of the spectra now become mixed up. Given the scan speed of the laser, only spectral diffusion on a time scale >200 ms is suppressed. The spectroscopic parameters associated with the $k = 0$ transition in these three complexes are listed in Table 1. The relative oscillator strength of the transition has been calculated by dividing its intensity by the total intensity observed in the B850 spectral region. The energy separation between the average spectral position of the $k = 0$ transition and that of the $k = \pm 1$ transitions is denoted by $\delta E_{01}$ and is given for each complex. Despite the poor statistics, the data in Table 1 suggest that the transition-dipole moment of the $k = 0$ state becomes stronger when the energy separation, $\delta E_{01}$, to the $k = \pm 1$ exciton states increases. This is in qualitative agreement with model calculations on this system (Monshouwer et al., 1997; Alden et al., 1997; Wu et al., 1997; Freiberg et al., 1999). The limited statistical information about the $k = 0$ state precludes any further conclusions, although in principle the intensity of this state provides an independent check of the intracomplex disorder (Mostovoy and Knoester, 2000).

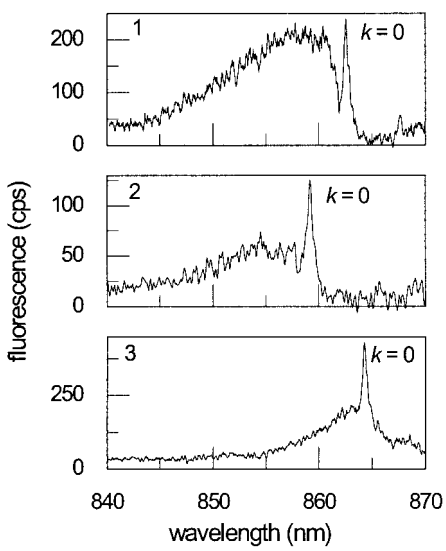


FIGURE 5 Fluorescence-excitation spectra of the long wavelength part of the B850 band of three different complexes (1–3), featuring a very narrow transition at the red wing of the $k = \pm 1$ absorptions. The spectra are obtained by a summation of repetitively scanned spectra at a high scan rate, where the $k = 0$ transitions are aligned before summation to correct for spectral diffusion (see text). Spectroscopic details are given in Table 1. The experimental conditions are the same as in Fig. 3.

**TABLE 1 Spectroscopic details of the $k = 0$ transitions of the three complexes depicted in Fig. 5**

| Complex (see Fig. 5) | Spectral position (nm) | FWHM* ($cm^{-1}$) | Relative oscillator strength† (%) | $\delta E_{01}$ ($cm^{-1}$) |
|---|---|---|---|---|
| 1 | 862.5 | 10 | 2 | 58 |
| 2 | 859.3 | 13 | 9 | 93 |
| 3 | 864.2 | 12 | 10 | 102 |

*Transition corrected for spectral diffusion.
†Oscillator strength relative to total oscillator strength of the B850 band.

For the energy separation between the $k = \pm 1$ states, $\delta E_{\pm 1}$, we obtain a distribution centered at 110 $cm^{-1}$. In order to ascertain that this splitting is not a matrix-induced effect, we performed additional experiments with LH2 dissolved in glycerol. For this matrix we observed a similar separation in energy for the two mutually orthogonal absorptions. Therefore, we conclude that the degeneracy of the $k = \pm 1$ exciton states is lifted by an intrinsic effect of the BChl *a* assembly.

## DISCUSSION

The gross features of the observations can be explained very well in terms of the exciton model for a circular aggregate of nine dimers as described above in the Theory section. The two prominent absorptions at 864 nm and 856 nm (Fig. 4 *b*) are assigned to the low energy $k = \pm 1$ exciton states. An important basis for this assignment is the observation that their transition-dipole moments are orthogonal and lie in the plane of the ring. Further support is found in the observation of the relatively narrow absorption line at the low energy side of the $k = \pm 1$ bands, which is assigned to the $k = 0$ exciton level. The absorption around 841 nm (Fig. 4 *b*) is attributed to higher exciton states. The lifting of the degeneracy of the $k = \pm 1$ states and the appreciable oscillator strength of the higher exciton states are ascribed to a perturbation of the circular symmetry of the LH2 complexes, which affects the site energies of and the intermolecular interactions between the individual BChl molecules.

To analyze our observations in more detail, we first consider the effect of random diagonal disorder on the properties of the exciton levels of the unperturbed ring of BChl *a* molecules. Random diagonal disorder in the site energies of the B850 pigments (Monshouwer et al., 1997; Alden et al., 1997; Hu et al., 1997; Wu and Small, 1998; Freiberg et al., 1999) leads to a redistribution of oscillator strength from the $k = \pm 1$ states preferentially to the adjacent exciton states, i.e., $k = 0$ and $k = \pm 2$ (Dracheva et al.,

1996). Consequently, we might assign the absorption around 841 nm to the $k = \pm 2$ exciton states. From the energy separation of 285 $cm^{-1}$ between the $k = \pm 1$ and the $k = \pm 2$ states, we can determine the interaction strength between the pigments using Eq. 2. If we assume that the second-neighbor interactions are all equal ($W_\alpha = W_\beta = \bar{W}$), $\bar{W} = -V_{avg}/8$, and $E_\alpha = E_\beta$, we obtain a value of 585 ± 35 $cm^{-1}$ for the average interaction strength ($V_{avg}$). This value is much larger than the interactions calculated theoretically which are found to be in the range of 200 to 400 $cm^{-1}$ (Sauer et al., 1996; Alden et al., 1997; Sundström et al., 1999; Freiberg et al., 1999; Scholes and Fleming, 2000). It appears that these values are relatively insensitive to the level of sophistication of the calculations. Although there is some spread in the calculated interaction energies, we conclude that assignment of the 841 nm band to the $k = \pm 2$ exciton states leads to a discrepancy between the experimentally determined interaction energy and the calculated values. In addition to this discrepancy, several other observations cannot be explained on the basis of purely random diagonal disorder. First, with the value for the interaction strength as derived above ($V_{avg}$ = 585 $cm^{-1}$), a random disorder of $\Gamma \sim 750$ $cm^{-1}$ is needed to explain an average splitting of 110 $cm^{-1}$ for the $k = \pm 1$ states (Fig. 2 *a*, lower part). Such a large disorder will lead to a strong broadening of the exciton manifold (Fig. 2 *a*, top part), and, as a result, the spectral width of the simulated ensemble spectrum would be significantly larger than that of the experimentally observed absorption spectrum. Secondly, random diagonal disorder affects all degenerate pairs of the exciton manifold in the same way (Fig. 2 *a*). In other words, a diagonal disorder sufficient to explain the splitting of the $k = \pm 1$ states also causes a splitting of 110 $cm^{-1}$ for the $k = \pm 2$, which is clearly not observed. Therefore, we conclude that the 841 nm band cannot be assigned to the $k = \pm 2$ exciton states and that an alternative explanation for the observed features of the electronic structure of LH2 must be considered.

In order to explain the splitting of the $k = \pm 1$ exciton states, we introduce a $C_2$-type modulation of the interaction between adjacent B850 pigments in LH2, which couples specifically exciton states that differ by $\Delta k = \pm 2$. In addition to lifting the degeneracy of the $k = \pm 1$ states, it leads to a transfer of oscillator strength from the $k = \pm 1$ to the $k = \pm 3$ states. Based on this conjecture, we assign the 841 nm absorption band to the $k = \pm 3$ exciton states. From this assignment we find for the average interaction strength a value of $V_{avg}$ = 240 ± 35 $cm^{-1}$ which gives $V_i$ = 254 ± 35 $cm^{-1}$ for the intradimer and $V_e$ = 225 ± 35 $cm^{-1}$ for the interdimer interaction if the ratio $V_e/V_i$ is calculated using the point-dipole approximation. These values are within the range of what is currently accepted (Sundström et al., 1999).

The $C_2$-type modulation of the interaction lifts the degeneracy of the $k = \pm 3$ states only in higher order. In view of the width of the lines and the signal-to-noise ratio of our spectra, we are not able to resolve the resulting small splitting of the $k = \pm 3$ band. However, as shown in Fig. 4 *a*, we do observe a slight polarization dependence of the intensity of this band.

Another indication for the presence of a $C_2$ modulation of the interaction is provided by the intensity ratio of the 856 nm and 864 nm bands. With purely random disorder, the average of this intensity ratio would be 1. We observe for most of the complexes that the intensity of the 864 nm band is larger than the intensity of the 856 nm band (Fig. 4 *a*). This result can be reproduced by assuming a structural deformation which leads to a $C_2$-type modulation of the interactions (see Matsushita et al., 2001).

To relate the $C_2$-type modulation of the interactions to the geometry of the transition moments, we introduce a structural deformation of the B850 ring. Since the leading term of the deformation of a circle into an ellipse has the same $\cos(2\theta)$ dependence as the $C_2$-type modulation, we restrict ourselves to an elliptical deformation in the plane of the ring. Different arrangements of the 18 pigments on an ellipse are possible. In the companion paper, three different arrangements of the 18 pigments on an ellipse are considered and compared to the experimental observations (Matsushita et al., 2001). It turned out that only one model could consistently describe the experimental observations. In this model (Model C in Matsushita et al., 2001), the interpigment distance on the ellipse is modulated in such a way that it is the longest at the long axis of the ellipse. This arrangement is generated by displacing each pigment along the line connecting the center of the ring and the position of the pigment in the unperturbed circle, retaining its geometrical angle $\theta$. To accommodate the deformation of the ring, the pigments were reoriented in such a way that the $Q_y$ transition moments preserved their angle with the local tangent of the ellipse. The interpigment interactions were approximated by a point-dipole interaction.

The effect of the deformation on the exciton states resembles that in Fig. 2 *b*, indicating that the deformation predominantly induces a $C_2$-type modulation in $V_{0,n}$ and $W_{0,n}$. The most pronounced effect of the deformation is the energy splitting of the $k = \pm 1$ states which exceeds that of the $k = \pm 2$ and $\pm 3$ states. To explain a $k = \pm 1$ splitting of 110 $cm^{-1}$ a deformation amplitude $\delta r/r_0 \simeq 7\%$ is required, where $r_0$ is the radius of the unperturbed ring and the long and short axes of the ellipse deviate from $r_0$ by $\delta r$ (Matsushita et al., 2001). The deformation causes a modulation in the center-to-center distance between nearest-neighbor pigments with an amplitude of ~0.66 Å (≃7%). This results in a modulation of the nearest-neighbor interaction energies with an amplitude of ~56 $cm^{-1}$ (≃22%). To retain the angle with the overall structure the transition moments had to be rotated in the *xy* plane of the complex by up to 7°. A value of $\delta r/r_0 \simeq 8\%$ is needed to get an intensity ratio 0.7 between the 856 nm and 864 nm bands (Matsushita et al., 2001). The mutual orthogonality of the transition-dipole

moments of the $k = \pm 1$ states is not significantly affected by this deformation, consistent with the experimental results. Thus, an elliptical deformation of $\delta r/r_0 = 7\%–8\%$ in a simple point-dipole approximation explains the major features of the single-molecule spectra, i.e., $\delta E_{\pm 1} = 110$ $cm^{-1}$ for the average $k = \pm 1$ splitting, the average intensity ratio of 0.7 between the 856 nm and 864 nm bands and their mutually orthogonal polarization.

Now we consider the effects of random disorder in addition to an elliptical deformation. It is seen from the histograms of Fig. 6, *a* and *b*, that the splitting $\delta E_{\pm 1}$ and the intensity ratio of the 856 and 864 nm bands vary from one complex to the other. Since the $C_2$-type modulation of the interactions alone would result in the same splitting of the $k = \pm 1$ states and of the intensity ratio of the 864 and 856 nm bands for all the complexes, these variations clearly indicate heterogeneity among the B850 pigments. Such heterogeneity is caused by random disorder that can exist in both the site energies of the pigments (random diagonal disorder) and/or their interactions (random off-diagonal disorder). Because $\delta E_{\pm 1}$ and the intensity ratio of the $k = \pm 1$ exciton states are determined by the disorder within one complex, these disorders should be considered as intracomplex disorder. Similarly, it can be expected that the amplitude of the elliptical deformation will be subjected to a distribution, which should be considered as intercomplex disorder. Since it is difficult to separate all the different types of heterogeneity we approximate the description of the heterogeneity in the B850 band by a two-step procedure. Firstly, we consider the character of the excited states of the individual complexes, which we assume to be determined by intracomplex disorder. In the second step we investigate the consequences that result for the ensemble of complexes when intercomplex disorder is taken into account.

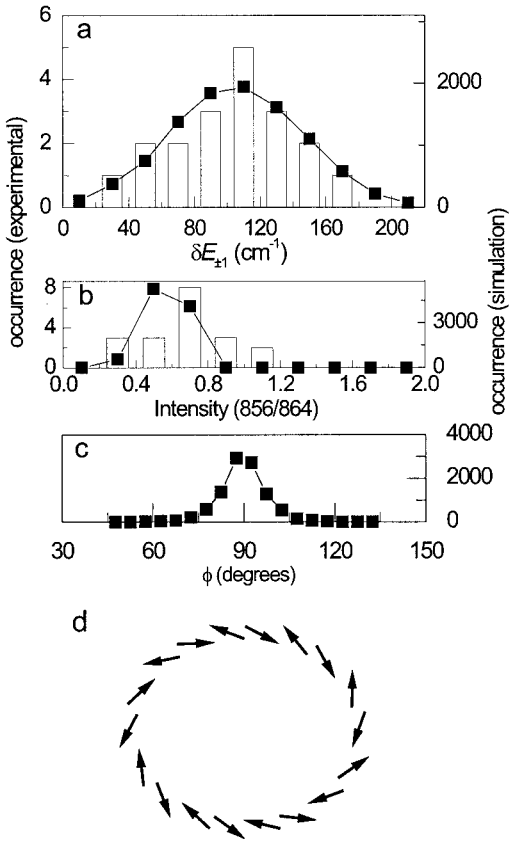


FIGURE 6 Comparison between the experimental distributions (*histograms*) and numerical simulations (*solid squares*). The experimental data refer to the left vertical scale and have been obtained at the same experimental conditions as given in Fig. 3. The numerical simulations refer to the right vertical scale and are based on the following parameters: $E_\alpha = 240$ $cm^{-1}$, $E_\beta = 0$ $cm^{-1}$, $V_i = 254$ $cm^{-1}$, $V_e = 226$ $cm^{-1}$, $W_\alpha = -35$ $cm^{-1}$, $W_\beta = -25$ $cm^{-1}$, amplitude of the elliptical deformation $\delta r/r_0 = 8.5\%$. For more details see text. (*a*) Energy separation of the two $k = \pm 1$ transitions. (*b*) Intensity ratio 864/856 of the two $k = \pm 1$ transitions. (*c*) Mutual angle between the $k = \pm 1$ transition-dipole moments. (*d*) The shape of the B850 ring, with the orientations of the molecular transition moments, with an elliptical deformation of $\delta r/r_0 = 8.5\%$.

To model the individual complexes, we fixed the amplitude of the elliptical deformation to a particular value and only random diagonal intracomplex disorder was included in the simulations. The result of these simulations are also presented in Fig. 6 and compared with the experimental data. The solid black squares in Fig. 6 *a* represent the result of a Monte Carlo simulation of the distribution of $\delta E_{\pm 1}$. The deformation amplitude is $\delta r/r_0 = 8.5\%$ and the intracomplex diagonal disorder ($\Gamma_{intra}$) has a FWHM of 250 $cm^{-1}$. It appears that the simulation fits the experimental distribution very well. The center of the distribution is largely determined by the amplitude of the elliptical deformation, but it is also influenced by the random disorder. The random disorder mixes the $k = 0$ state with the lower component of the $k = \pm 1$ states, by which oscillator strength is transferred to the $k = 0$ state. At the same time, the lower component of the $k = \pm 1$ states shifts to higher energy, making the separation between the $k = \pm 1$ states smaller. Thus, the center of the $\delta E_{\pm 1}$ distribution will be shifted to a smaller value than in the absence of random disorder. Accordingly, the deformation amplitude derived from the simulation, which includes random disorder, is slightly larger than the previously mentioned 7%.

The width of the $\delta E_{\pm 1}$ distribution in Fig. 6 *a* is determined mainly by the random diagonal disorder. The value of 250 $cm^{-1}$ sets an upper value for the random diagonal disorder, because the experimentally observed distribution includes contributions from other types of heterogeneity, which are neglected in the simulation. The results of the simulation of the distribution of the intensity ratio between the 856 and 864 nm bands is shown by the solid black squares in Fig. 6 *b*. In the simulation the intensity of the $k = 0$ state is included in that of the 864 nm band, since in most of the complexes the narrow $k = 0$ band is hidden under the broad 864 nm band, and is not distinguishable due to its rapid spectral diffusion. The simulation gives reasonable agreement with the experimental distribution. Fig. 6 *c*

shows the simulated distribution of the angle between the two transition-dipoles of the $k = \pm 1$ states. The geometry of the 18 $Q_y$ transition dipoles in an elliptically deformed ring with $\delta r/r_0 = 8.5\%$ is shown in Fig. 6 *d*.

The 250 $cm^{-1}$ random diagonal intracomplex disorder will not only split the $k = \pm 1$ degenerate states, but also all other pairs of degenerate levels. When introducing both random diagonal intracomplex disorder and a fixed elliptical deformation, the simulations predict a distribution of splittings of the $k = \pm 3$ states centered on 40 $cm^{-1}$ (results not shown). These splittings are caused by both the higher order terms of the elliptical deformation as well as the $C_3$ symmetric component of the random diagonal disorder. In our experimental data we did not find clear evidence for such a large splitting. This could have two reasons. First, the random diagonal disorder is $<250$ $cm^{-1}$, since it is very likely that the LH2 complexes also show a distribution of amplitudes of the elliptical deformation that will contribute to the width of the distribution of Fig. 6 *a*. As a result, the splitting of the $k = \pm 3$ states may be $<40$ $cm^{-1}$. Second, the signal-to-noise ratio of the $k = \pm 3$ bands in most of the spectra was relatively poor, making it very difficult to observe a splitting.

The value of 250 $cm^{-1}$ FWHM for the random diagonal disorder in the B850 band of LH2 in a PVA film is smaller than the values reported by other authors (Sundström et al., 1999). With this value for the diagonal disorder, some structure remains in the simulation of the experimentally observed B850 band of a bulk sample. In Fig. 7, the calculated and the observed spectra are shown, and it is seen that the splitting between the two components of the $k = \pm 1$ states, induced by the elliptical deformation and random disorder, is still visible in the simulated curve (*dashed line*) in contrast to the observed spectrum. The reason for this apparent discrepancy is that the value of 250 $cm^{-1}$ for the heterogeneity obtained from the $k = \pm 1$ splitting reflects only the heterogeneity within individual complexes (intracomplex disorder). In order to describe the ensemble spectrum, the sample heterogeneity or intercomplex disorder should also be included (Freiberg et al., 1999; van Oijen et al., 2000). Such heterogeneity originates from the slightly different environments of the different LH2 complexes in the host matrix.

From the distribution of the spectral lines observed in the B850 band (Fig. 4 *b*) it is not possible to find an accurate value for the intercomplex diagonal disorder, since the spectral positions depend not only on the site energies of the pigments, but also on their interactions. For the B800 band this is not the case, since the interactions are relatively weak compared to the diagonal disorder (van Oijen et al., 1998). Therefore, a good estimate for the intercomplex diagonal disorder of the B850 pigments is obtained from the variation in spectral mean in the B800 band of each LH2 complex. For the B800 band, a value of 120 $cm^{-1}$ FWHM was found (van Oijen et al., 2000). Taking the same value for the intercomplex diagonal disorder of the B850 band, we performed the Monte Carlo simulation of the ensemble spectrum. The result is shown in Fig. 7 (*dotted line*). The simulation nicely reproduces the experimentally measured ensemble spectrum, which indicates that both inter- and intracomplex disorder are relevant.

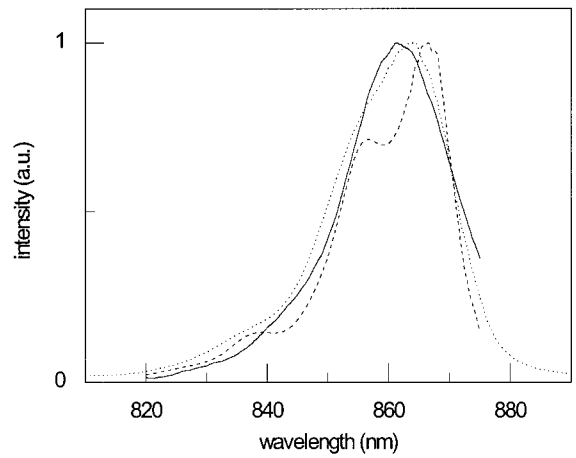


FIGURE 7 Comparison between the experimental, low-temperature ensemble spectrum of LH2 (*solid line*) and two simulated spectra. The experimental ensemble spectrum lacks the long-wavelength tail, because of overlap with the fluorescence detection window. For both simulated spectra the deformation amplitude $\delta r/r_0 = 8.5\%$. *Dashed line*: only intracomplex heterogeneity is taken into account. *Dotted line*: both, intra- and intercomplex heterogeneity, are included in the simulation, with $\Gamma_{intra} = 250$ $cm^{-1}$ and $\Gamma_{inter} = 120$ $cm^{-1}$. The individual transitions have homogeneous Lorentzian line shapes with a width (FWHM) of 100 $cm^{-1}$ ($k \neq 0$) and 10 $cm^{-1}$ ($k = 0$). The parameters used for the unperturbed B850 ring are $E_\alpha = 12{,}300$ $cm^{-1}$, $E_\beta = 12{,}060$ $cm^{-1}$, $V_i = 254$ $cm^{-1}$, $V_e = 226$ $cm^{-1}$, $W_\alpha = -35$ $cm^{-1}$, $W_\beta = -25$ $cm^{-1}$.

The direct insight into both the inter- and intracomplex disorder of an ensemble of single LH2 complex has important implications for the discussion on the delocalization length in these type of systems. Bakalis and Knoester (2000) discussed the determination of the delocalization length from the width of the ensemble-averaged absorption spectrum. Since the intercomplex disorder does not affect the delocalization length, whereas it does contribute to the width of the ensemble-averaged spectrum, this will lead to an underestimation of the delocalization length through this method. A similar reasoning applies to the value for the delocalization length as determined by transient absorption spectroscopy (Bakalis and Knoester, 1999). In a recent paper, Mostovoy and Knoester (2000) point out that the existence of intercomplex disorder gives rise to an underestimation of the delocalization length, and they stress the potential power of single-aggregate experiments to determine this parameter.

Because the sum of the spectra from the individual complexes and the fluorescence-detected ensemble spectrum are in very good agreement (Fig. 3, top trace), the individual complexes studied so far are representative of the com-

plexes as studied by bulk fluorescence measurements. The question arises whether fluorescence detection is selective for complexes that have a large $k = \pm 1$ splitting, i.e., have a large $C_2$-symmetric component in their overall disorder.

Clearly, the detection method is most sensitive to complexes that have a relatively strong transition-dipole moment in the $k = 0$ exciton state from which the fluorescence is emitted. As was already mentioned in the theory section, the $k = 0$ state gains oscillator strength due to mixing with the $k = \pm 1$ states. Such a mixing is invoked by random disorder in the system. As was pointed out by Wu and Small (1997), it is only the $C_1$-symmetric component of this disorder that causes the mixing. The splitting of the $k = \pm 1$ states is not affected by this component, since these states can only be split by a $C_2$-type of disorder. *A priori* there is no correlation between the amplitudes of the $C_1$ and $C_2$ components of random disorder. Therefore, no correlation between the oscillator strength of the $k = 0$ state and the splitting of the $k = \pm 1$ states is expected. This is in agreement with our model calculations, where diagonal disorder is introduced in the range of $0 < \Gamma/V \leq 4$ (result not shown). Hence, we rule out the possibility that the fluorescence detection of single complexes is selective for those which have a large $k = \pm 1$ splitting.

## CONCLUSIONS

The results presented in this paper show that single-molecule spectroscopic techniques at cryogenic temperatures can be applied successfully to elucidate the electronic structure of photosynthetic pigment-protein complexes. The advantage of the method is that effects of ensemble averaging, which are typical for conventional forms of spectroscopy, are eliminated. We conclude that the B850 assembly of BChl *a* pigments in LH2 represents a strongly coupled system, and that the electronic properties are appropriately described as Frenkel excitons. The observations are consistent with alternating nearest neighbor interaction energies of $254 \pm 35$ cm$^{-1}$ and $225 \pm 35$ cm$^{-1}$, respectively, with a distribution of site energies (diagonal disorder) given by a FWHM of 250 cm$^{-1}$. These parameters imply that the optical excitations are largely delocalized over the ring of BChl *a* pigments (Mostovoy and Knoester, 2000). In addition to the random diagonal disorder, a $C_2$-type modulation of the intermolecular interaction must be assumed to account for the relative intensities and the spectral positions of the exciton transitions. This modulation is most probably caused by a structural deformation of the LH2 complex, which transforms the B850 ring from a circular to an elliptical geometry.

It is not surprising that our experimental results cannot be interpreted on the basis of an exciton model for a perfect circular aggregate of nine dimers. Already the ensemble measurements (Sundström et al., 1999) and single-molecule experiments (Bopp et al., 1997; Tietz et al., 1999; van Oijen et al., 1999a) on the spectroscopy of LH2 indicate the presence of disorder in this system. It is generally believed that the origin of such disorder is the random variation in the site energies of the pigments involved (Sundström et al., 1999). However, also random differences in the coupling between the pigments have been suggested (Sturgis and Robert, 1997). The randomness of such disorder has very specific implications for the exciton manifold, but this alone is not sufficient to describe our experimental observations consistently. Based on the additional assumption of a $C_2$-type modulation of the interactions, we suggest that the B850 ring is transformed from a perfect in-plane isotropic absorber and emitter into an elliptic one. Other groups have also found evidence for this anisotropic emitting behavior of single LH2 complexes at room temperature and low temperature, using either mica plates or polymer films to immobilize the complexes (Tietz et al., 1999; Bopp et al., 1999). The modulation of the interaction between the pigments most probably is related to a geometrical distortion of the LH2 ring. Bopp et al. (1999) showed that the anisotropic behavior of single LH2 complexes at room temperature could be explained very well by an elliptical deformation of the LH2 ring, which varies in time. Such a temporal variation of the ellipticity cannot be observed at 1.2 K, where the complexes presumably are trapped in local minima of the potential energy surface, each corresponding to a distinct orientation of the elliptical deformation.

The reduced symmetry of the isolated LH2 complexes at low temperature and at room temperature is at odds with the ninefold symmetry of LH2 in crystalline form. It might be that the dense packing of LH2 complexes in the crystal provides a stabilizing force that is absent in the isolated complexes, as already suggested by van Oijen et al. (1999a). The question of whether or not the static deformation is representative for the structure of LH2 in detergent solution or in membranes remains to be answered. Experiments are in progress to study this aspect in more detail. Nevertheless, this does not significantly affect our conclusions about (static) disorder, the strength of the intermolecular interactions, and the delocalization of optical excitations over the ring. Static disorder is a result of the variation of site energies, and this variation depends on very local conformation parameters. The interaction strength is determined by intermolecular distances and the average of the modulated interactions in our model correspond to that of a fully symmetric LH2 ring. Delocalization at low temperature (1.2 K) is determined by the degree of static disorder with respect to the interaction strength. At higher temperatures thermally induced effects will dominate, and dynamic electron-phonon coupling will lead to a fast hopping-type motion of localized excitations. From the present experiments we have derived a basic framework for the electronic structure of LH2, and the parameters that we have obtained should be considered in describing the properties of LH2 at room temperature in detergent solution as well as in vivo.

We thank J. P. Abrahams (Leiden University, Leiden, the Netherlands), J. Knoester (Groningen University, Groningen, the Netherlands), and J. H. van der Waals (Leiden University) for helpful discussions. We also thank D. de Wit for the preparation of the LH2 complexes and M. Hesselberth for assistance with the spin-coating.

This work is part of the research program of the Stichting voor Fundamenteel Onderzoek der Materie (FOM) with financial aid from the Nederlandse Organisatie voor Wetenschappelijk Onderzoek (NWO) and is further supported by the Section Earth and Life Sciences (ALW) of the Netherlands Organization for Scientific Research (NWO) and by the Volkswagen-Stiftung (Germany, Hannover).

*Note:* We have recently learned that the results of our numerical simulations of the single LH2 spectra are confirmed by an analysis of the data by Mostovoy and Knoester (2000). If we translate the parameters used by these authors to our notation, they find a best fit for an elliptical deformation of $\delta r/r_0 \sim 7.5\%$ and $\Gamma_{\text{intra}} = 235\ \text{cm}^{-1}$. They also conclude that a consistent interpretation of the spectra is possible only if intercomplex disorder is included ($\Gamma_{\text{inter}} = 150\ \text{cm}^{-1}$). These numbers agree very well with our numerical simulations. In addition, they estimated the oscillator strength of the $k = 0$ state to be 3.5 to 10% of the total oscillator strength of the B850 band, which is consistent with our observations.

## REFERENCES

Alden, R. G., E. Johnson, V. Nagarajan, W. W. Parson, C. J. Law, and R. J. Cogdell. 1997. Calculations of spectroscopic properties of the LH2 bacteriochlorophyll-protein antenna complex from *Rhodopseudomonas acidophila*. *J. Phys. Chem. B.* 101:4667–4680.

Bakalis, L. D., and J. Knoester. 1999. Pump-probe spectroscopy and the exciton delocalization length in molecular aggregates. *J. Phys. Chem. B* 103:6620–6628.

Bakalis, L. D., and J. Knoester. 2000. Lineair absorption as a tool to measure the exciton delocalization length in molecular assemblies. *J. Lumin.* 87–89:66–70.

Beekman, L. M. P., R. N. Frese, G. J. S. Fowler, R. Picorel, R. J. Cogdell, I. H. M. van Stokkum, C. N. Hunter, and R. van Grondelle. 1997. Characterization of the light-harvesting antennas of photosynthetic purple bacteria by stark spectroscopy. 2. LH2 complexes: influences of the protein environment. *J. Phys. Chem. B.* 101:7293–7301.

Bopp, M. A., J. Yiwei, L. Li, R. J. Cogdell, and R. M. Hochstrasser. 1997. Fluorescence and photobleaching dynamics of single light-harvesting complexes. *Proc. Natl. Acad. Sci. USA.* 94:10630–10635.

Bopp, M. A., A. Sytnik, T. D. Howard, R. J. Cogdell, and R. M. Hochstrasser. 1999. The dynamics of structural deformations of immobilized single light-harvesting complexes. *Proc. Natl. Acad. Sci. USA.* 96: 11271–11276.

Cantor, C. R., and P. R. Schimmel. 1980. Techniques for the Study of Biological Structure and Function. W.H. Freeman and Company, San Francisco.

Chachisvilis, M., O. Kühn, T. Pullerits, and V. Sundström. 1997. Excitons in photosynthetic purple bacteria: wavelike motion or incoherent hopping? *J. Phys. Chem. B.* 101:7275–7283.

De Caro, C., R. Visscher, R. van Grondelle, and S. Volker. 1994. Inter- and intraband energy transfer in LH2-antenna complexes of purple bacteria: a fluorescence line-narrowing and hole-burning study. *J. Phys. Chem.* 98:10584–10590.

Dracheva, T. V., V. I. Novoderezhkin, and A. P. Razjivin. 1996. Site inhomogeneity and exciton delocalization in the photosynthetic antenna. *Photosynth. Res.* 49:269–276.

Du, M., X. L. Xie, L. Mets, and G. R. Fleming. 1994. Direct observation of ultrafast energy-transfer processes in light harvesting complex II. *J. Phys. Chem.* 98:4736–4741.

Fidder, H., J. Knoester, and D. A. Wiersma. 1991. Optical properties of disordered molecular aggregates: a numerical study. *J. Chem. Phys.* 95:7880–7890.

Freiberg, A., K. Timpmann, R. Ruus, and N. W. Woodbury. 1999. Disordered exciton analysis of linear and nonlinear absorption spectra of antenna bacteriochlorophyll aggregates: LH2-only mutant chromatophores of Rhodobacter sphaeroides at 8 K under spectrally selective excitation. *J. Phys. Chem. B.* 103:10032–10041.

Hess, S., F. Feldchtein, A. Babin, I. Nurgaleev, T. Pullerits, A. Sergeev, and V. Sundström. 1993. Femtosecond energy transfer within the LH2 peripheral antenna of the photosynthetic purple bacteria *Rhodobacter sphaeroides* and *Rhopseudomonas palustris* LL. *Chem. Phys. Lett.* 216: 247–257.

Hu, X., T. Ritz, A. Damjanovic, and K. Schulten. 1997. Pigment organization and transfer of electronic excitation in the photosynthetic unit of purple bacteria. *J. Phys. Chem. B.* 101:3854–3871.

Jimenez, R., F. van Mourik, J. Y. Yu, and G. R. Fleming. 1997. Three-pulse photon echo measurment on LH1 and LH2 complexes of *Rhodobacter sphaeroides*: a nonlinear spectroscopic probe of energy transfer. *J. Phys. Chem. B.* 101:7350–7359.

Joo, T., Y. Jia, J.-Y. Yu, D. M. Jonas, and G. R. Fleming. 1996. Dynamics in isolated bacterial light harvesting antenna (LH2) of *Rhodobacter sphaeroides* at room temperature. *J. Phys. Chem.* 100:2399–2409.

Kennis, J. T. M., A. M. Streltsov, S. I. E. Vulto, T. J. Aartsma, T. Nozawa, and J. Amesz. 1997a. Femtosecond dynamics in isolated LH2 complexes of various species of purple bacteria. *J. Phys. Chem. B* 101:7827–7834.

Kennis, J. T. M., A. M. Streltsov, H. Permentier, T. J. Aartsma, and J. Amesz. 1997b. Exciton coherence and energy transfer in the LH2 complex of *Rhodopseudomonas acidophila* at low temperature. *J. Phys. Chem. B.* 101:8369–8374.

Koolhaas, M. H. C., G. van der Zwan, R. N. Frese, and R. van Grondelle. 1997. Red shift of the zero crossing in the cd spectra of the LH2 antenna complex of *Rhodopseudomonas acidophila*: a structure-based study. *J. Phys. Chem. B.* 101:7262–7270.

Koolhaas, M. H. C., R. N. Frese, G. J. S. Fowler, T. S. Bibby, S. Georgakopoulou, G. van der Zwan, C. N. Hunter, and R. van Grondelle. 1998. Identification of the upper exciton component of the B850 bacteriochlorophylls of the LH2 antenna complex, using a B800-free mutant of *Rhodobacter sphaeroides*. *Biochemistry.* 37:4693–4698.

Krueger, B. P., G. D. Scholes, and G. R. Fleming. 1998. Calculation of couplings and energy-transfer pathways between the pigments of LH2 by the *ab initio* transition density cube method. *J. Phys. Chem. B* 102:5378–5386.

Lösche, M., G. Feher, and Y. M. Okamura. 1987. The stark effect in reaction centers from *Rhodobacter sphaeroides* R-26 and *Rhodopseudomonas viridis*. *Proc. Natl. Acad. Sci. USA.* 84:7537–7541.

Matsushita, M., M. Ketelaars, A. M. van Oijen, J. Köhler, T. J. Aartsma, and J. Schmidt. 2001. Spectroscopy on the B850 band of individual light-harvesting 2 complexes of *Rhodopseudomonas acidophila*. II. Exciton states of an elliptically deformed ring aggregate. *Biophys. J.* 80:1604–1614.

McDermott, G., S. M. Prince, A. A. Freer, A. M. Hawthornthwaite-Lawless, M. Z. Papiz, R. J. Cogdell, and N. W. Isaacs. 1995. Crystal structure of an integral membrane light-harvesting complex from photosynthetic bacteria. *Nature.* 374:517–521.

Monshouwer, R., I. Ortiz de Zarate, F. van Mourik, and R. van Grondelle. 1995. Low-intensity pump-probe spectroscopy on the B800 to B850 transfer in the light harvesting 2 complex of *Rhodobacter sphaeroides*. *Chem. Phys. Lett.* 246:341–346.

Monshouwer, R., and R. van Grondelle. 1996. Excitation and excitons in bacterial light-harvesting complexes. *Biochim. Biophys. Acta.* 1275: 70–75.

Monshouwer, R., M. Abrahamsson, F. van Mourik, and R. van Grondelle. 1997. Superradiance and exciton delocalisation in bacterial photosynthetic light-harvesting systems. *J. Phys. Chem. B* 101:7241–7248.

Mostovoy, M. V., and J. Knoester. 2000. Statistics of optical spectra from single ring-aggegates and its aplication to LH2. *J. Phys. Chem. B.* 104:12355–12364.

Novoderezhkin, V. I., R. Monshouwer, and R. van Grondelle. 1999. Exciton (de)localization in the LH2. antenna of Rhodobacter sphaeroides as revealed by relative difference absorption measurements of the LH2 antenna and the B820 subunit. *J. Phys. Chem. B.* 103:10540–10548.

Polivka, T., T. Pullerits, J. L. Herek, and V. Sundström 2000. Exciton relaxation and polaron formation in LH2 at low temperature. *J. Phys. Chem. B.* 104:1088–1096.

Pullerits, T., M. Chachisvilis, M. R. Jones, C. N. Hunter, and V. Sundström. 1994. Exciton dynamics in the light-harvesting complexes of Rhodobacter sphaeroides. *Chem. Phys. Lett.* 224:355–365.

Pullerits, T., M. Chachisvilis, and V. Sundström. 1996. Exciton delocalization length in the B850 antenna of *Rhodobacter sphaeroides*. *J. Phys. Chem.* 100:10787–10792.

Sauer, K., R. J. Cogdell, S. M. Prince, A. A. Freer, N. W. Isaacs, and H. Scheer. 1996. Structure-based calculations of the optical spectra of the LH2 bacteriochlorophyll-protein complex from *Rhodopseudomonas acidophila. Photochem. Photobiol.* 64:564–576.

Scholes, G. D., I. R. Gould, R. J. Cogdell, and G. R. Fleming. 1999. Ab initio molecular orbital calculations of electronic couplings in the LH2 bacterial light-harvesting complex of *Rps. acidophila. J. Phys. Chem. B.* 103:2543–2553.

Scholes, G. D., and G. R. Fleming. 2000. On the mechanism of light harvesting in photosynthetic purple bacteria: B800 to B850 energy transfer. *J. Phys. Chem. B.* 104:1854–1868.

Sturgis, J. N., and B. Robert. 1997. Pigment binding-site and electronic properties in light-harvesting proteins of purple bacteria. *J. Phys. Chem. B.* 101:7227–7231.

Sundström, V., T. Pullerits, and R. van Grondelle. 1999. Photosynthetic light-harvesting: reconciling dynamics and structure of purple bacterial LH2 reveals function of photosynthetic unit. *J. Phys. Chem. B.* 103: 2327–2346.

Tietz, C., O. Chekhlov, A. Dräbenstedt, J. Schuster, and J. Wrachtrup. 1999. Spectroscopy on single light-harvesting complexes at low temperature. *J. Phys. Chem. B.* 103:6328–6333.

van Oijen, A. M., M. Ketelaars, J. Köhler, T. J. Aartsma, and J. Schmidt. 1998. Spectroscopy of single light-harvesting complexes from purple photosynthetic bacteria at 1.2 K. *J. Phys. Chem. B.* 102:9363–9366.

van Oijen, A. M., M. Ketelaars, J. Köhler, T. J. Aartsma, and J. Schmidt. 1999a. Unraveling the electronic structure of individual photosynthetic pigment-protein complexes. *Science.* 285:400–402.

van Oijen, A. M., M. Ketelaars, J. Köhler, T. J. Aartsma, and J. Schmidt. 1999b. Spectroscopy of individual LH2 complexes of *Rhodopseudomonas acidophila*: localized excitations in the B800 band. *Chem. Phys.* 247:53–60.

van Oijen, A. M., M. Ketelaars, J. Köhler, T. J. Aartsma, and J. Schmidt. 2000. Spectroscopy of individual LH2 complexes of *Rhodopseudomonas acidophila*: diagonal disorder, intercomplex heterogeneity, spectral diffusion, and energy transfer in the B800. *Biophys. J.* 78:1570–1577.

Vulto, S. I. E., M. A. de Baat, S. Neerken, F. R. Nowak, H. van Amerongen, J. Amesz, and T. J. Aartsma. 1999a. Excited state dynamics in FMO antenna complexes from photosynthetic green sulfur bacteria: a kinetic model. *J. Phys. Chem. B.* 103:8153–8161.

Vulto, S. I. E., J. T. M. Kennis, A. M. Streltsov, J. Amesz, and T. J. Aartsma. 1999b. Energy relaxation within the B850 absorption band of the isolated light-harvesting complex LH2 from *Rhodopseudomonas acidophila* at low temperature. *J. Phys. Chem. B.* 103:878–883.

Wu, H.-M., M. Ratsep, I.-J. Lee, R. J. Cogdell, and G. J. Small. 1997. Exciton level structure and energy disorder of the B850 ring in the LH2 antenna complex. *J. Phys. Chem. B.* 101:7654–7663.

Wu, H.-M., and G. J. Small. 1997. Symmetry adapted basis defect pattern for analysis of the effects of energy disorder on cyclic arrays of coupled chromophores. *Chem. Phys.* 218:225–234.

Wu, H.-M., and G. J. Small. 1998. Symmetry-based analysis of the effects of random energy disorder on the excitonic level structure of cyclic arrays: application to photosynthetic antenna complexes. *J. Phys. Chem. B.* 102:888–898.

Zhao, Y., T. Meier, W. M. Zhang, V. Chernyak, and S. Mukamel. 1999. Superradiance coherence sizes in single-molecule spectroscopy of LH2 antenna complexes. *J. Phys. Chem. B.* 103:3954–3962.